

Electron Withdrawing Substituents on Equatorial and Apical Phosphines Have Opposite Effects on the Regioselectivity of Rhodium Catalyzed Hydroformylation

Charles P. Casey,* Evelyn Lin Paulsen, Eckart W. Beuttenmueller, Bernd R. Proft, Lori M. Petrovich, Brock A. Matter, and Douglas R. Powell

Contribution from the Department of Chemistry, University of Wisconsin, Madison, Wisconsin 53706

Received June 12, 1997[⊗]

Abstract: The electronic effects of electron withdrawing aryl substituents on equatorial and apical diphosphines were investigated. Chelating diphosphines designed to coordinate in diequatorial or in apical–equatorial positions were synthesized, and their effects on the regioselectivity of rhodium catalyzed 1-hexene hydroformylation were observed. Only diequatorial coordination was observed for 2,2'-bis[(diphenylphosphino)methyl]-1,1'-biphenyl (BISBI) complexes (BISBI)Ir(CO)₂H (**8**) and [BISBI-(3,5-CF₃)]Ir(CO)₂H (**10**), and only apical–equatorial coordination was seen for 1,2-bis(diphenylphosphino)ethane (DIPHOS) complexes (DIPHOS)Ir(CO)₂H (**14**) and [DIPHOS-(3,5-CF₃)]Ir(CO)₂H (**15**). For the *trans*-1,2-bis[(diphenylphosphino)methyl]cyclopropane (T-BDCP) complexes, a mixture of diequatorial and apical–equatorial complexes was seen. For (T-BDCP)Ir(CO)₂H (**12**), **12-ae** was favored over **12-ee** by 63:37, but for [T-BDCP-(3,5-CF₃)]Ir(CO)₂H (**13**) the conformational preference was reversed and a 10:90 ratio of **13-ae**:**13-ee** was seen. The electron withdrawing groups in the equatorial positions of BISBI-(3,5-CF₃) (**1**) and T-BDCP-(3,5-CF₃) (**2**) led to an increase in *n*-aldehyde regioselectivity in rhodium catalyzed hydroformylation. However, electron withdrawing aryl substituents in the apical positions of DIPHOS-(3,5-CF₃) (**3**) led to a decrease in *n*-aldehyde regioselectivity in rhodium catalyzed hydroformylation.

The hydroformylation reaction¹ employing very efficient homogeneous rhodium-phosphine catalysts, first developed by Wilkinson² and first implemented by Union Carbide,³ is one of the most important industrial uses of homogeneous catalysis. These catalysts are important because they are highly regioselective for the desired linear (*n*) aldehyde over branched (*i*) aldehyde and require lower temperatures and pressures than earlier cobalt-based catalysts. Control of the regiochemistry of the hydroformylation of terminal alkenes remains a focus of industrial research. Recent success in achieving high *n*:*i* ratios of aldehydes include Texas Eastman's use of the 2,2'-bis-[(diphenylphosphino)methyl]-1,1'-biphenyl (BISBI) ligand⁴ and Union Carbide's development of diphosphite chelates.⁵ Stanley has developed a unique binuclear rhodium catalyst that gives high rates and selectivity.⁶ van Leeuwen has reported a variety of diphosphite and diphosphine ligands that give high *n*:*i*

regioselectivity.⁷ Buchwald⁸ and Wink⁹ have obtained high regioselectivities in hydroformylation of functionalized alkenes using rhodium diphosphite systems. While extensive screening of a wide variety of phosphine and phosphite ligands has been reported, no detailed understanding of how phosphines control regioselectivity or enantioselectivity has emerged.

In Wilkinson's dissociative hydroformylation mechanism (Scheme 1), aldehyde regioselectivity is determined in the hydride addition step that converts a five-coordinate H(alkene)-Rh(CO)L₂ into either a primary or secondary four-coordinate (alkyl)Rh(CO)L₂. To understand and control regioselectivity, it is important to know the detailed structure of the key five-coordinate H(alkene)Rh(CO)L₂ intermediate. Two monodentate phosphine ligands might occupy two equatorial or one equatorial and one apical site in a trigonal bipyramidal intermediate. For L = PPh₃, Brown's NMR studies showed an 85:15 diequatorial:apical–equatorial mixture of isomers of (PPh₃)₂Rh(CO)₂H which are in rapid equilibrium at room temperature.¹⁰

Several years ago we set out to test the hypothesis that very different regioselectivities might be obtained from diequatorial

[⊗] Abstract published in *Advance ACS Abstracts*, November 15, 1997.

(1) (a) Parshall, G. W. *Homogeneous Catalysis: The Applications and Chemistry of Catalysis by Soluble Transition Metal Complexes*; Wiley: New York, 1980. (b) Tkatchenko, I. In *Comprehensive Organometallic Chemistry*; Wilkinson, G., Stone, F. G. A., Abel, E. W., Eds.; Pergamon: Oxford, 1982; Vol. 8, pp 101–223. (c) Tolman, C. A.; Faller, J. W. In *Homogeneous Catalysis with Metal Phosphine Complexes*; Pignolet, L. H., Ed.; Plenum: New York, 1983; pp 81–109. (d) Pino, P.; Piacenti, F.; Bianchi, M. In *Organic Syntheses via Metal Carbonyls*; Wender, I., Pino, P., Eds.; Wiley Interscience: New York, 1977; Vol. 2, pp 136–197. (e) Consiglio, G.; Pino, P. *Top. Curr. Chem.* **1982**, 105, 77. (f) Beller, M.; Cornils, B.; Frohning, C. D.; Kohlpaintner, C. W. *J. Mol. Catal. A* **1995**, 104, 17–85.

(2) (a) Evans, D.; Osborn, J. A.; Wilkinson, G. *J. Chem. Soc. A* **1968**, 3133. (b) Yagupsky, G.; Brown, C. K.; Wilkinson, G. *J. Chem. Soc. A* **1970**, 1392. (c) Brown, C. K.; Wilkinson, G. *J. Chem. Soc. A* **1970**, 2753.

(3) Pruett, R. L. *Ann. N. Y. Acad. Sci.* **1977**, 295, 239.

(4) (a) Devon, T. J.; Phillips, G. W.; Puckette, T. A.; Stavinoha, J. L.; Vanderbilt, J. J. (to Texas Eastman) U.S. Patent 4,694,109, **1987**; *Chem. Abstr.* **1988**, 108, 7890. For closely related systems, see: (b) Devon, T. J.; Phillips, G. W.; Puckette, T. A.; Stavinoha, J. L.; Vanderbilt, J. J. (to Texas Eastman) U.S. Patent 5,332,846, **1994**; *Chem. Abstr.* **1994**, 121, 280, 879. (c) Bahrmann, H.; Lappe, P.; Herrmann, W. A.; Albanese, G. P.; Manetsberger, R. B. (to Hoechst AG) DE Patent 4,333,307, **1995**; *Chem. Abstr.* **1995**, 123, 112,408.

(5) (a) Billig, E.; Abatjoglou, A. G.; Bryant, D. R. (to Union Carbide) U.S. Patent 4,748,261 **1988**; 4,769,498 **1988**. (b) For related work with phosphine-phosphite chelates, see: Nozaki, K.; Sakai, N.; Nanno, T.; Higashijima, T.; Mano, S.; Horiuchi, T.; Takaya, H. *J. Am. Chem. Soc.* **1997**, 119, 4413.

(6) Broussard, M. E.; Juma, B.; Train, S. G.; Peng, W.-J.; Laneman, S. A.; Stanley, G. G. *Science* **1993**, 260, 1784.

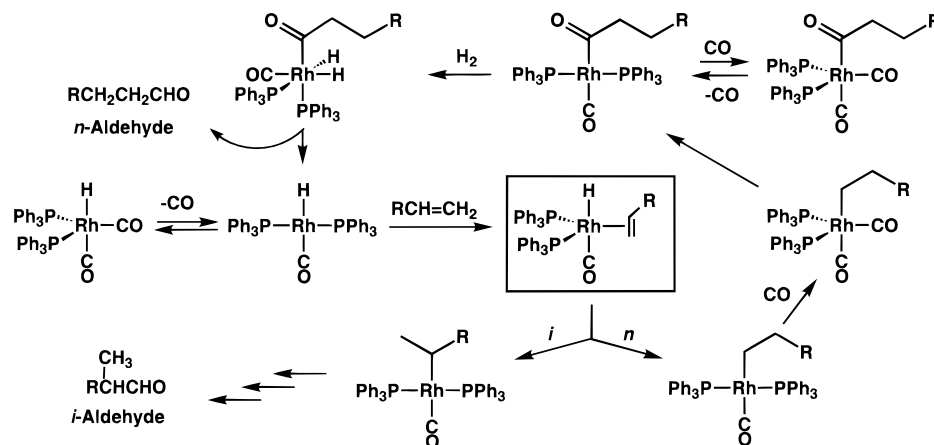
(7) (a) van Rooy, A.; Kamer, P. C. J.; van Leeuwen, P. W. N. M.; Goubitz, K.; Fraanje, J.; Veldman, N.; Spek, A. L. *Organometallics* **1996**, 15, 835. (b) Buisman, G. J. H.; Martin, M. E.; Vos, E. J.; Klootwijk, A.; Kamer, P. C. J.; van Leeuwen, P. W. N. M. *Tetrahedron: Asymmetry* **1995**, 6, 719. (c) Kranenburg, M.; van der Burgt, Y. E. M.; Kamer, P. C. J.; van Leeuwen, P. W. N. M.; Goubitz, K.; Fraanje, J. *Organometallics* **1995**, 14, 3081.

(8) Cuny, G. D.; Buchwald S. L. *J. Am. Chem. Soc.* **1993**, 115, 2066.

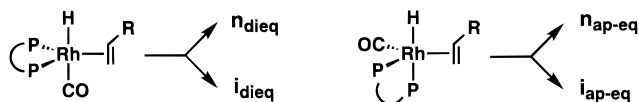
(9) Kwok, T. J.; Wink, D. J. *Organometallics* **1993**, 12, 1954.

(10) Brown, J. W.; Kent, A. G. *J. Chem. Soc., Perkin Trans. II* **1987**, 1597.

Scheme 1



Scheme 2



diphosphine rhodium complexes and from apical–equatorial diphosphine rhodium complexes (Scheme 2). In the course of testing this hypothesis, we carried out molecular mechanics calculations on a number of diphosphine chelates to determine their “natural bite angle” and the flexibility of the bite angle.¹¹ Chelates with wide natural bite angles near 120° were chosen to achieve preferential diequatorial coordination, and chelates with narrow bite angles near 90° were chosen to achieve apical–equatorial coordination. A strong correlation was found between regioselectivity for *n*-aldehyde formation and natural bite angle.¹² Chelates like BISBI with wide natural bite angles gave a much higher % *n*-aldehyde ($\beta_n = 113^\circ$, $n:i = 66$) than diphosphines like 1,2-bis(diphenylphosphino)ethane (DIPHOS) with narrow bite angles ($\beta_n = 85^\circ$, $n:i = 2.6$).^{13,14} X-ray structures of (BISBI)Rh(PPh₃)(CO)H and (BISBI)Ir(CO)₂H indicated that BISBI is coordinated diequatorially.¹² DIPHOS is coordinated in an apical–equatorial manner in five-coordinate (DIPHOS)Fe(CO)₃¹⁵ as well as in (DIPHOS)Ir(CO)₂H.¹⁶ Deuterioformylation studies established that the predominant products were derived from irreversible addition of a rhodium hydride to a complexed alkene to give a rhodium alkyl intermediate that is committed to aldehyde formation.¹⁷

The correlation between regioselectivity and chelation mode suggests that diequatorial diphosphines like BISBI and apical–equatorial chelating diphosphines like DIPHOS have either significantly different steric or electronic properties. We first considered the steric differences between diequatorial and apical–equatorial chelates as a possible explanation for regio-

selectivity. In particular, we looked for a special role for flexible wide bite angle diphosphines in promoting formation of linear products.

Molecular mechanics calculations were employed to explore whether selectivity arose from steric differences between the transition states leading to the primary and secondary alkyl–rhodium intermediates.¹⁷ The steric energy difference between the transition state models leading to (BISBI)Rh(*n*-propyl)(CO) and (BISBI)Rh(*i*-propyl)(CO) was calculated to be 1.9 kcal mol⁻¹ favoring the *n*-propyl transition state. This energy difference corresponds to a 25:1 partitioning between *n*- and isopropyl rhodium intermediates, in reasonable agreement with the 66:1 *n:i* aldehyde selectivity observed in hydroformylation with BISBI which corresponds to 2.5 kcal mol⁻¹. However, the calculated steric energy difference between the transition state models leading to (DIPHOS)Rh(*n*-propyl)(CO) and (DIPHOS)Rh(isopropyl)(CO) was even larger, 2.1 kcal mol⁻¹ also favoring the *n*-propyl transition state. This energy difference corresponds to 35:1 *n:i* selectivity, a value much higher than the observed DIPHOS selectivity of 2.6:1, which requires an energy difference of only 0.6 kcal mol⁻¹. These estimates of steric effects incorrectly suggested that DIPHOS should be more selective than BISBI, which is in fact the opposite of the trend observed.

Since steric arguments failed to give a satisfactory explanation for the much higher *n:i* aldehyde ratios observed from diequatorial chelates like BISBI compared with apical–equatorial chelates like DIPHOS, we must consider whether the electronic differences between diequatorial chelates and apical–equatorial chelates are responsible for the differences in regioselectivity. Because the electronic interaction between two apical ligands or between two equatorial ligands is stronger than the interaction between apical and equatorial ligands, electronic differences can be expected between diequatorial chelated complexes and apical–equatorial chelated complexes. For example, back bonding from rhodium to the alkene ligand in the equatorial plane would be expected to be stronger for the BISBI complex with two strong donor phosphines in the equatorial plane than for the DIPHOS complex with only a single donor phosphine in the equatorial plane. Also, the apical hydride of the BISBI complex is trans to a CO ligand and would be expected to be more acidic than the hydride of the DIPHOS complex which is trans to a phosphine.

To investigate electronic effects of equatorial and apical phosphines, we have synthesized analogs of our chelating diphosphines having electron withdrawing substituents on the aryl rings and measured the resulting changes in hydroformylation regioselectivity. Here we report that the introduction of

(11) Casey, C. P.; Whiteker, G. T. *Isr. J. Chem.* **1990**, *30*, 299.

(12) Casey, C. P.; Whiteker, G. T.; Melville, M. G.; Petrovich, L. M.; Gavney, J. A., Jr.; Powell, D. R. *J. Am. Chem. Soc.* **1992**, *114*, 5535.

(13) van Leeuwen also observed an increase in linear aldehyde regioselectivity with increasing bite angle.^{7c} In a series of bidentate chelating phosphines containing xanthene-like ligand backbones, the bite angle was varied from 102° to 131° , with minimal change in the steric or electronic properties of the ligand. The resulting *n:i* ratio increased from 6.7 to 80.5 in the hydroformylation of 1-octene at 80°C .

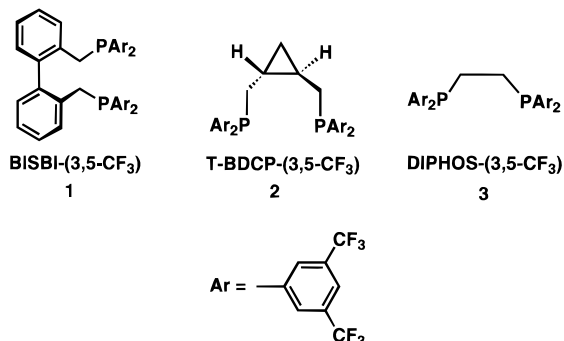
(14) Earlier¹² we reported a 2.1:1 *n:i* ratio for DIPHOS, which is the ratio seen early in the reaction. For consistency, we are now reporting ratios obtained after 120–250 turnovers (20–50% conversion) for all ligands.

(15) Battaglia, L. P.; Delledonne, D.; Nardelli, M.; Pelizzi, C.; Predieri, G.; Chiusoli, G. P. *J. Organomet. Chem.* **1987**, *330*, 101.

(16) (a) Fisher, B. J.; Eisenberg, R. *Organometallics* **1983**, *2*, 764. (b) Fisher, B. J.; Eisenberg, R. *Inorg. Chem.* **1984**, *23*, 3216.

(17) Casey, C. P.; Petrovich, L. M. *J. Am. Chem. Soc.*, **1995**, *117*, 6007.

electron withdrawing substituents on the aryl rings of the diequatorial chelate BISBI-(3,5-CF₃) (**1**) leads to an increase in linear aldehyde selectivity as well as rate. In contrast, introduction of electron withdrawing substituents on the aryl rings of the apical–equatorial chelate DIPHOS-(3,5-CF₃) (**3**) resulted in a decrease in linear aldehyde selectivity when compared with the phenyl-substituted DIPHOS.

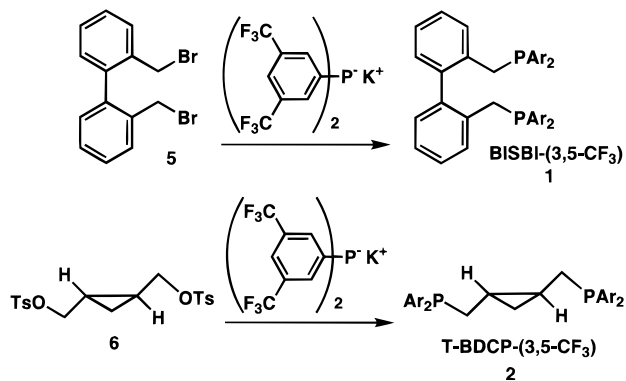


Results

Synthesis of Diphosphines with Electron Withdrawing Substituents. The reaction of the potassium phosphide derived from [3,5-(CF₃)₂C₆H₃]₂PH (**4**) with the appropriate dihalide or ditosylate was used to synthesize diphosphines having electron withdrawing aryl substituents. **4** was prepared by reduction of [3,5-(CF₃)₂C₆H₃]₂PCl¹⁸ with LiAlH₄ and subsequently converted to the phosphide by treatment with KH.

Addition of the phosphide derived from **4** to 2,2'-bis(bromomethyl)-1,1'-biphenyl (**5**) produced BISBI-(3,5-CF₃) (**1**) in 54% yield (Scheme 3). The ³¹P NMR resonance of **1**

Scheme 3



appeared at δ -8.5, shifted 2 ppm to higher frequency than BISBI. Similarly, the reaction of the potassium phosphide derived from **4** with the cyclopropane ditosylate **6** gave the corresponding *trans*-cyclopropane diaryldiphosphine T-BDCP-(3,5-CF₃) (**2**) in 36% yield. The ³¹P NMR resonance of **2** at δ -14.6 was also shifted to higher frequency by 5 ppm compared with the diphenyldiphosphine analog T-BDCP (*trans*-1,2-bis[(diphenylphosphino)methyl]cyclopropane).

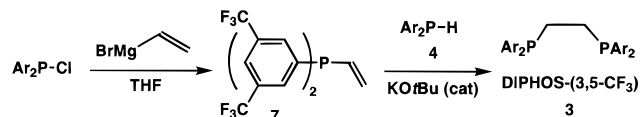
1,2-Bis(diarylmethyl)ethane derivatives were synthesized by base catalyzed addition of the secondary aryl phosphine **4** to a functionalized diarylvinyldiphosphine (Scheme 4).^{19–21} The vinyl phosphine [3,5-(CF₃)₂C₆H₃]₂PCH=CH₂ (**7**) was prepared

(18) Casalnuovo, A. L.; RajanBabu, T. V.; Ayers, T. A.; Warren, T. H. *J. Am. Chem. Soc.* **1994**, *116*, 9869.

(19) (a) Clark, P. W.; Mulraney, B. J. *J. Organomet. Chem.* **1981**, *217*, 51. (b) Chatt, J.; Hussain, W.; Leigh, G. J.; Ali, H. M.; Pickett, C. J.; Rankin, D. A. *J. Chem. Soc., Dalton Trans.* **1985**, 1131.

(20) The *o*-tolyl and (*o*-trifluoromethyl)phenyl substituted DIPHOS derivatives were synthesized by the same method. See Supporting Information.

Scheme 4



by addition of vinylmagnesium bromide to [3,5-(CF₃)₂C₆H₃]₂-PCl. The KO-*t*-Bu catalyzed coupling of **4** and **7** led to the isolation of 1,2-bis{bis[3,5-di(trifluoromethyl)phenyl]phosphino}ethane (**3**) in 52% yield. The ³¹P NMR resonance of **3** at δ -10.7 was shifted to higher frequency by 2 ppm compared with the parent DIPHOS.

Synthesis of Iridium Complexes as Models for Catalytic Species. The regioselectivity of aldehyde formation is determined by the partitioning of a chelating diphosphine rhodium hydride alkene complex between linear and branched alkyl rhodium species (Scheme 1). These intermediates have never been directly observed due to rapid conversion to acyl rhodium species. Possible models for these intermediates would be chelating diphosphine rhodium dicarbonyl hydrides, but in many cases such complexes are unstable relative to loss of hydrogen and dimer formation. For example, attempts to synthesize (T-BDCP)Rh(CO)₂H led to [(T-BDCP)Rh]₂(μ -CO)₂.¹² We have employed related iridium dicarbonyl hydride complexes to probe the chelation geometry of the five-coordinate metal center of the catalytically important rhodium hydride alkene complexes. Iridium and rhodium have similar coordination geometries, and iridium bond lengths are only 1–2% longer than related rhodium bond lengths.

BISBI Complexes. The X-ray crystal structure of (BISBI)-Ir(CO)₂H (**8**) shows a trigonal bipyramidal geometry with the chelating diphosphine occupying diequatorial sites with a bite angle of 117.9°. In the IR spectrum of **8**, bands were observed at 2074 cm⁻¹ (w, ν_{IrH}), 1985 (s, sym ν_{CO}), and 1932 (s, asym ν_{CO}) cm⁻¹. At -125 °C, two ³¹P{¹H} NMR doublets were seen for the diastereotopic phosphines at δ 10.6 ($J_{\text{PP}} = 107$ Hz) and -0.7 ($J_{\text{PP}} = 107$ Hz). A Berry pseudorotation process interchanges the environments of the phosphorus and causes coalescence of the phosphorus resonances at higher temperature. At room temperature, a singlet at δ 4.3 is seen. In the ¹H NMR spectrum at -125 °C, the Ir-H appears as a triplet coupled equally to two phosphorus atoms at δ -12.15 (t, $J_{\text{HP}} = 20$ Hz). Evidently, the diastereotopic phosphines have identical coupling constants to the *cis*-hydride.

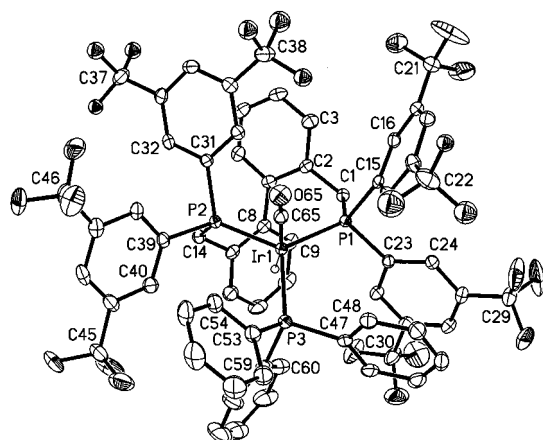
Initially, we attempted to prepare the BISBI-(3,5-CF₃) analog of iridium dicarbonyl complex **8** by first preparing [BISBI-(3,5-CF₃)]Ir(PPh₃)(CO)H (**9**) and then converting it to the dicarbonyl complex [BISBI-(3,5-CF₃)]Ir(CO)₂H (**10**). The reaction of BISBI-(3,5-CF₃) (**1**) with (PPh₃)₃Ir(CO)H in THF produced **9** in 80% yield. The X-ray structure of **9** indicates a trigonal bipyramidal structure with the chelating ligand occupying equatorial sites with a P–Ir–P angle of 118.20 (5)° (Figure 1). The carbonyl ligand occupies an apical position with a Ph₃P–Ir–CO angle of 94.6°, indicating that the Ir is distorted slightly toward the carbonyl ligand. Although the hydride was not located, we believe it occupies an apical site *trans* to CO. The structure of **9** is very similar to that of the related rhodium complex (BISBI)Rh(PPh₃)(CO)H¹² and supports the hypothesis that iridium complexes are excellent structural models for rhodium complexes (Table 1).

The presence of a hydride ligand in **9** was established by ¹H NMR spectroscopy, which showed a triplet of doublets at δ

(21) This synthesis route was designed in order to also have access to unsymmetrically substituted 1,2-bis(diarylmethyl)ethane derivatives (Ar₂PCH₂CH₂PAr'₂) via the use of differently substituted secondary phosphines and diarylvinyldiphosphines.

Table 1. Comparison of Bond Lengths (Å) and Angles (deg) of [BISBI-(3,5-CF₃)Ir(PPh₃)(CO)H (**9**), (BISBI)Rh(PPh₃)(CO)H·CH₂Cl₂,¹² and (BISBI)Ir(CO)₂H·1/2O(CHMe₂)₂¹²

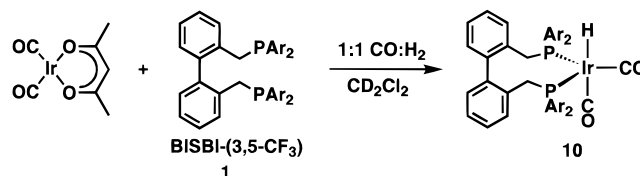
[BISBI-(3,5-CF ₃)Ir(PPh ₃)(CO)H (9)		(BISBI)Rh(PPh ₃)(CO)H		(BISBI)Ir(CO) ₂ H	
Bond Lengths (Å)					
Ir–P(1)	2.277 (1)	Rh–P(1)	2.285 (1)	Ir–P(1)	2.306 (3)
Ir–P(2)	2.270 (1)	Rh–P(2)	2.318 (1)	Ir–P(2)	2.300 (3)
Ir–P(3)	2.319 (1)	Rh–P(3)	2.318 (1)	Ir–C(1CO)	1.89 (1)
Ir–C(65)O	1.906 (6)	Rh–C(57)O	1.895 (5)	Ir–C(2CO)	1.90 (1)
Bond Angles (deg)					
P(1)–Ir–P(2)	118.20 (5)	P(1)–Rh–P(2)	124.8 (1)	P(1)–Ir–P(2)	117.9 (1)
P(1)–Ir–P(3)	117.18 (5)	P(1)–Rh–P(3)	122.6 (1)	P(1)–Ir–C(2CO)	93.4 (4)
P(2)–Ir–P(3)	120.19 (5)	P(2)–Rh–P(3)	108.0 (1)	P(2)–Ir–C(2CO)	98.3 (4)
P(1)–Ir–C(65)	100.2 (2)	P(1)–Rh–C(57)	95.3 (1)	P(1)–Ir–C(1CO)	125.8 (4)
P(2)–Ir–C(65)	96.4 (2)	P(2)–Rh–C(57)	93.3 (1)	P(2)–Ir–C(1CO)	112.2 (4)
P(3)–Ir–C(65)	94.6 (2)	P(3)–Rh–C(57)	103.1 (1)		

**Figure 1.** X-ray crystal structure of [BISBI-(3,5-CF₃)](PPh₃)Ir(CO)H (**9**).

–11.52 (td, $J_{HP} = 25, 20$ Hz). The relatively small H–P coupling constants are consistent with a structure containing an apical hydride coupled to three cis equatorial phosphines. The ³¹P NMR spectrum of **9** consisted of a complex ABC line pattern with more than eight lines between δ 12 and 16.

The BISBI dicarbonyl iridium hydride complex **8** was formed by bubbling CO through a solution of (BISBI)Ir(PPh₃)(CO)H.¹² However, when CO was bubbled through a solution of **9**, attempts to isolate the desired dicarbonyl compound failed, resulting instead in reisololation of starting material. Therefore the following alternative synthesis was devised.

[BISBI-(3,5-CF₃)Ir(CO)₂H (**10**) was prepared from the reaction of BISBI-(3,5-CF₃) (**1**) and Ir(acac)(CO)₂ in CD₂Cl₂ under 1 atm of 1:1 CO:H₂. In the IR spectrum of **10** in CH₂Cl₂ the Ir–H stretch at (w, 2079 cm^{–1}) and carbonyl stretches (2005 (s), and 1960 (vs) cm^{–1}) are all shifted to higher frequency than in the unsubstituted BISBI complex **8**. The electron withdrawing CF₃ groups in **9** make the phosphines poorer donors to iridium and leads to a reduction in backbonding from iridium to the CO ligands. At –84 °C, the ³¹P{¹H} NMR spectrum showed an AB quartet (δ 13.28 and 6.40, $J_{PP} = 122$ Hz) for the diastereotopic phosphines. In the ¹H NMR spectrum, the iridium hydride appeared at δ –12.54 (dd, $J_{HP} = 25, 15$ Hz) and showed inequivalent coupling to two phosphines. At room temperature a fluxional process interchanged the environments of the phosphines; a single ³¹P NMR resonance was observed at δ 9.2, and the ¹H NMR resonance of the iridium hydride (δ –12.32, t, $J_{HP} = 20$ Hz) showed averaged coupling to two phosphines. The room temperature J_{HP} of 20 Hz is the average of the two low temperature coupling constants.



T-BDCP Complexes. The 107° calculated natural bite angle of the T-BDCP ligand lies between the ideal 90° angle of an apical–equatorial chelate and the ideal 120° angle of a diequatorial chelate. The only X-ray crystal structure of a T-BDCP chelate is for (T-BDCP)Fe(CO)₃, which has a P–Fe–P bite angle of 123.9°.²² While this wide angle is close to the expected 120° bite angle for diequatorial chelation, it does not imply that T-BDCP is a selective diequatorial ligand since nonchelated (R₃P)₂Fe(CO)₃ compounds show an electronic preference for a wide P–Fe–P bite angles. For example, (Ph₃P)₂Fe(CO)₃ has a P–Fe–P angle of 173°.²³ (BISBI)Fe(CO)₃ has an unusually large bite angle of 152° compared with other BISBI complexes.²² Clearly, it is important to determine experimentally whether T-BDCP coordinates to iridium as a apical–equatorial chelate or a diequatorial chelate or a mixture of chelates.

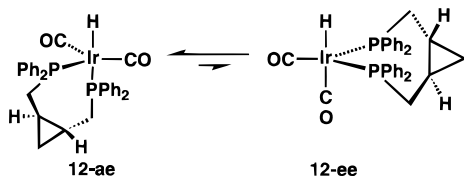
The reaction of T-BDCP with (PPh₃)₃Ir(CO)H in CH₂Cl₂ produced (T-BDCP)Ir(PPh₃)(CO)H (**11**) as a bright yellow solid in 80% yield. In the ¹H NMR spectrum of **11** in CD₂Cl₂, the iridium hydride appeared at δ –11.51 (ddd, $J_{HP} = 25.5, 21.5, 19.5$ Hz). The ³¹P{¹H} NMR spectrum of **11** in CD₂Cl₂ consisted of an AMX pattern due to complexed PPh₃ and the two diastereotopic phosphines of the T-BDCP ligand (δ 15.3, 11.0, 10.2; $J_{PP} = 133, 126, 126$ Hz). These coupling patterns are consistent with a trigonal bipyramidal structure with three equatorial phosphines. Apparently, the relatively bulky phosphine ligands prefer to chelate equatorially to minimize steric interactions.

(T-BDCP)Ir(CO)₂H (**12**) was synthesized in 66% yield by reaction of (T-BDCP)Ir(PPh₃)(CO)H (**11**) with CO. The low temperature ¹H and ³¹P NMR spectra of **12** in CD₂Cl₂ provided evidence for a 3.3:1 ratio of isomers. In the ¹H NMR spectrum –74 °C, the metal hydride resonance of the major isomer appeared as a doublet of doublets at δ –12.07 (dd, $J_{HP} = 97, –23$ Hz).²⁴ This isomer was assigned the apical–equatorial chelate configuration **12-ae** based on the observation of a large coupling between an apical hydride and an apical phosphorus

(22) Casey, C. P.; Whiteker, G. T.; Campana, C. F.; Powell, D. R. *Inorg. Chem.* **1990**, *29*, 3376.

(23) Glaser, R.; Yoo, Y.-H.; Chen, G. S.; Barnes, C. L. *Organometallics* **1994**, *13*, 2578.

and a small coupling between the hydride and an equatorial phosphorus. The ^{31}P NMR spectrum of **12-ae** showed two different phosphorus doublets at δ 0.93 (d, $J_{\text{PP}} = 24$ Hz) and -5.15 (d, $J_{\text{PP}} = 24$ Hz), tentatively assigned to the equatorial and apical phosphines, respectively. The hydride resonance of the minor isomer appeared at δ -11.35 ($J_{\text{HP}} = -26, -15$ Hz). This isomer was assigned a diequatorial chelate configuration **12-ee** based on the observation of two small couplings between an apical hydride and diastereotopic equatorial phosphines. In the ^{31}P NMR spectrum of **12-ee**, the two diastereotopic equatorial phosphines had similar chemical shifts and showed stronger coupling (δ 7.25 and 5.34, $J_{\text{PP}} = 105$ Hz). Coupling constants between diequatorial phosphines are generally larger than couplings between equatorial and apical phosphines. The IR spectrum of the mixture of **12-ae** and **12-ee** in hexane confirms the existence of two dicarbonyl species, showing carbonyl bands at 1990(s), 1978(s), 1943(vs), and 1930(vs) cm^{-1} .

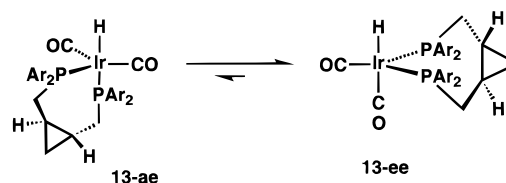


At room temperature, the two isomers, **12-ae** and **12-ee**, rapidly interconvert, and all phosphorous environments are interchanged, presumably by a Berry pseudorotation mechanism. In the room temperature $^{31}\text{P}\{^1\text{H}\}$ NMR, a singlet at δ 1.3 was observed. In the room temperature ^1H NMR spectrum, a single hydride resonance was observed at δ -11.48 (t, $J = 16$ Hz). Assuming the coupling constants do not vary with temperature, the ratio of **12-ae:12-ee** at 25 °C can be calculated using the coupling constants in the formula $J_{\text{RT}} = \chi_{\text{ee}}(J_{\text{ee}})_{\text{avg}} + (1 - \chi_{\text{ee}})(J_{\text{ae}})_{\text{avg}}$ where $J_{\text{RT}} =$ coupling at 25 °C = 16 Hz; $(J_{\text{ee}})_{\text{avg}} =$ average coupling of **12-ee** at -74 °C = $(-26 + -15) \div 2 = -20.5$ Hz; $(J_{\text{ae}})_{\text{avg}} =$ average coupling of **12-ae** at -74 °C = $(97 + -23) \div 2 = 37$ Hz; $\chi_{\text{ee}} =$ fraction of **12-ee** at 25 °C; and $\chi_{\text{ae}} = 1 - \chi_{\text{ee}} =$ fraction of **12-ae** at 25 °C. The solution to the equation gives a 63:37 ratio of **12-ae:12-ee** at room temperature.²⁵

[T-BDCP-(3,5- CF_3)] $\text{Ir}(\text{CO})_2\text{H}$ (**13**) was prepared from the reaction of T-BDCP-(3,5- CF_3) (**2**) and $\text{Ir}(\text{acac})(\text{CO})_2$ in CD_2Cl_2 under 1 atm of CO/H_2 .²⁶ In contrast to (T-BDCP) $\text{Ir}(\text{CO})_2\text{H}$ (**12**) where a 63:37 ratio of apical–equatorial isomer **12-ae**:diequatorial isomer **12-ee** was observed, only the diequatorial isomer of [T-BDCP-(3,5- CF_3)] $\text{Ir}(\text{CO})_2\text{H}$, **13-ee**, was observed by low temperature ^1H and ^{31}P NMR spectroscopy. None of the apical–equatorial isomer was observed, and as little as 5% would have been easily detected. In the ^1H NMR spectrum of **13** in CD_2Cl_2 at -84 °C, the hydride resonance at δ -12.3 (dd, $J_{\text{HP}} = -28, -17$ Hz) showed two small phosphorus couplings. In the $^{31}\text{P}\{^1\text{H}\}$ NMR spectrum at -84 °C, an AB quartet was observed at δ 13.06 and 10.78 ($J_{\text{PP}} = 116$ Hz) with large coupling between the equatorial phosphines. The small

H–P coupling constants of -17 and -28 Hz suggest that the diastereotopic phosphines are cis to the hydride, consistent with a diequatorial chelation. The large P–P coupling constant is observed when phosphines are in the diequatorial position of these five-coordinate iridium complexes. The IR spectrum at room temperature in CH_2Cl_2 showed an Ir–H stretch at 2064 cm^{-1} and broad carbonyl bands at 2001 (s) and 1955 (vs) cm^{-1} ; because the carbonyl bands are broad, it is not possible to tell whether a second isomer is present. These IR frequencies are shifted to higher frequencies indicating a reduction in back bonding compared to the diphenyl substituted complex.

At room temperature, a rapid fluxional process interchanges the environment of the phosphine ligands, and a single $^{31}\text{P}\{^1\text{H}\}$ NMR resonance is observed at δ 11.34. In the ^1H NMR, a triplet is seen at δ -12.03 (t, $J_{\text{HP}} = 16.5$ Hz). If the diequatorial isomer **13-ee** were the only species present, then the coupling constant would have been -22.5 Hz, the average of the coupling constants seen for **13-ee** at -84 °C. We attribute the smaller observed coupling to the presence of a small amount of the apical–equatorial isomer **13-ae**, which should have coupling constants similar to those of **12-ae** ($J_{\text{HP}} = 97, -23$ Hz). Using calculations similar to those for **12-ae:12-ee**, the observed coupling is consistent with a 10:90 mixture of **13-ae:13-ee**.



The electron-withdrawing CF_3 substituents on T-BDCP-(3,5- CF_3) shift the equilibrium between diequatorial and apical–equatorial isomers toward the diequatorial isomer compared with the unsubstituted T-BDCP complexes. Hoffmann's molecular orbital analysis of ligand electronic site preferences in five coordinate d^8 ML_5 complexes²⁷ suggested that σ donor ligands should prefer the apical position while σ -acceptor ligands should prefer the equatorial position. The electron-withdrawing CF_3 substituents make T-BDCP-(3,5- CF_3) a better σ -acceptor ligand (and weaker σ -donor ligand); this explains the shift in the equilibrium toward diequatorial coordination upon introduction of the CF_3 substituents.

DIPHOS Complexes. The calculated natural bite angle of DIPHOS is 84.5° and bite angles of $84 \pm 4^\circ$ were found in a sampling of 20 X-ray structures from the Cambridge data base. DIPHOS would therefore be expected to span apical and equatorial sites in a trigonal bipyramid. (DIPHOS) $\text{Ir}(\text{CO})_2\text{H}$ (**14**) was synthesized by a procedure similar to that reported by Eisenberg¹⁶ (see Supporting Information). The room temperature ^1H and ^{31}P NMR spectra of **14** were previously reported by Eisenberg; a hydride with equal coupling to two phosphines was seen at δ -11.20 (t, $J_{\text{HP}} = 40$ Hz), and a single phosphorus resonance was observed at δ 32.5.

Our low temperature NMR studies establish that DIPHOS chelates in an apical–equatorial fashion in **14**. At -79 °C, the ^1H NMR spectrum shows the Ir–H coupled to two different phosphorus atoms (dd, $J_{\text{HP}} = 92, -13$ Hz), and the $^{31}\text{P}\{^1\text{H}\}$ NMR spectrum shows two doublets ($J_{\text{PP}} = 10$ Hz) at δ 33.2 and 31.3. The $^{13}\text{C}\{^1\text{H}\}$ NMR spectrum at -79 °C exhibited a doublet at δ 173.5 ($J_{\text{CP}} = 24$ Hz) for the equivalent equatorial

(24) These coupling constants must have opposite signs to explain the average 16 Hz coupling seen for the fluxional mixture of isomers at room temperature. Similar coupling constants were assigned to $(\text{R}_3\text{P})_2(\text{CO})_2\text{IrH}$: (a) Meakin, P.; Muetterties, E. L.; Jesson, J. P. *J. Am. Chem. Soc.* **1972**, *94*, 5271. (b) Yagupsky, G.; Wilkinson, G. *J. Chem. Soc. A* **1969**, 725.

(25) Mathematical solution of this equation gives two ratios depending on whether the observed coupling is 16 or -16 Hz. If the coupling is 16 Hz, **12-ae:12-ee** = 63:37 and if the coupling is -16 Hz, **12-ae:12-ee** = 8:92. The later ratio would require that the major species at -74 and 25 °C be different.

(26) Attempts to prepare **13** from [T-BDCP-(3,5- CF_3)] $\text{Ir}(\text{CO})(\text{PPh}_3)\text{H}$ failed. See Supporting Information.

(27) Rossi, A. R.; Hoffmann, R. *Inorg. Chem.* **1975**, *14*, 365.

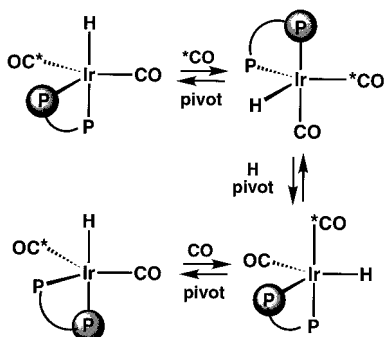
Table 2. Regiochemistry of Hydroformylation of 1-Hexene with Rhodium Diphosphine Catalysts

diphosphine	ee:ae ^a	aldehyde n:i ^b	regiochemistry %n	turnover rate ^c
BISBI	100:0	66.5 ± 0.5	98.52 ± 0.02	12.4 ± 0.7
BISBI-(3,5-CF ₃) (1)	100:0	123 ± 3	99.20 ± 0.02	61.9 ± 2.6
T-BDCP	37:63	12.1 ± 0.4	92.4 ± 0.2	3.7 ± 0.1
T-BDCP-(3,5-CF ₃) (2)	90:10	17.7 ± 0.3	94.7 ± 0.1	13.7 ± 0.4
DIPHOS	0:100	2.6 ± 0.1	71.9 ± 0.3	3.5 ± 0.1
DIPHOS-(3,5-CF ₃) (3)	0:100	1.3 ± 0.1	56.9 ± 0.9	4.3 ± 0.1

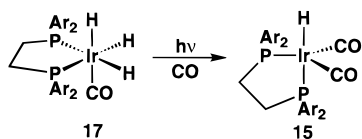
^a Ratio of diequatorial:apical–equatorial chelates of (diphosphine)Ir(CO)₂H at room temperature. ^b Mol heptanal:mol 2-methylhexanal. ^c Turnover rate = [mol aldehyde] × [mol Rh]⁻¹ h⁻¹.

CO ligands. These data unequivocally establishes the apical–equatorial coordination of DIPHOS ligand in **14**.²⁸

The fluxional process that exchanges the environment of the DIPHOS phosphorus atoms of **14** at room temperature is probably also a Berry pseudorotation.



[DIPHOS-(3,5-CF₃)]Ir(CO)₂H (**15**) was synthesized in several steps starting from NBU₄⁺Ir(CO)₂I₂⁻ (**16**).²⁹ Reaction of DIPHOS-(3,5-CF₃) (**3**) with **16** followed by reduction with NaBH₄ in ethanol gave *fac*-[DIPHOS-(3,5-CF₃)]Ir(CO)H₃ (**17**) in 57% yield. Photolysis of **17** under CO gave [DIPHOS-(3,5-CF₃)]Ir(CO)₂H (**15**).



Room temperature ¹H NMR showed a triplet at -10.90 ppm in the hydride region with $J_{HP} = 44$ Hz. As in the DIPHOS complex above, an average value of P–H coupling constant of 44 Hz suggests the existence of some type of fluxional process interconverting the apical and equatorial phosphorus atoms, making them equivalent. In the ¹H NMR spectrum of **15** at -110 °C, the hydride resonance appeared as a doublet of doublets at $\delta -10.97$ ($J_{HP} = 101, -14$ Hz). Two phosphine resonances at $\delta 39.0$ and 37.5 were observed in the ³¹P{¹H} NMR spectrum of **15** at -96 °C. When all but the hydride resonance was decoupled, a broad singlet at $\delta 39.15$ and a broad doublet at $\delta 37.4$ ($J_{HP} = 103$ Hz) were observed. These coupling patterns are consistent with a conformation having an apical hydride with a large coupling to an apical phosphine and a small coupling to an equatorial phosphine.

At room temperature, a fluxional process interchanges the environments of the phosphines, and a single ³¹P{¹H} NMR resonance was observed at $\delta 39.8$ and the hydride resonance appeared as a triplet at $\delta 10.09$ with $J_{PH} = 44$ Hz. Note that this coupling constant is the average of the couplings at low temperature and supports the contention that J_{HP} is temperature independent that was used in estimating the ratio of **12-ae:12-ee** and **13-ae:13-ee** at room temperature. The average room

temperature coupling constant of 44 Hz for **15** requires opposite signs for the large and small J_{HP} couplings seen at low temperature.

Coalescence of the phosphorus resonances occurred at -88 °C. This allowed calculation of $\Delta G^\ddagger = 8.6$ kcal mol⁻¹ for a fluxional process that interconverts the environments of the phosphine groups,³⁰ presumably involving a series of Berry pseudorotations.

Summary of Coordination Geometries. Only diequatorial coordination is observed for BISBI complexes **8** and **10**, and only apical–equatorial coordination is seen for DIPHOS complexes **14** and **15**. For the T-BDCP complexes, a mixture of diequatorial and apical–equatorial complexes is seen. For (T-BDCP)Ir(CO)₂H (**12**), a 63:37 ratio of **12-ae:12-ee** was estimated at room temperature. Electron withdrawing aryl groups of [T-BDCP-(3,5-CF₃)]Ir(CO)₂H reversed the conformational preference, and a 10:90 ratio of **13-ae:13-ee** was estimated at room temperature.

Catalytic Hydroformylation of 1-Hexene. Hydroformylation of 1-hexene was carried out in a benzene solution at 36 °C under 6 atm of 1:1 H₂:CO using 0.2 mol % 1:1 Rh:diphosphine catalyst prepared from Rh(CO)₂(acac) and the chelating diphosphine. The production of heptanal and 2-methylhexanal was monitored by gas chromatography utilizing toluene as an internal standard. The results of the studies are summarized in Table 2.³¹ The turnover rate and n:i ratios are reported after 120–250 turnovers (20–50% conversion).

The wide bite angle diphosphine BISBI occupies diequatorial sites in (diphosphine)Ir(CO)₂H and (diphosphine)Rh(CO)₂H¹² complexes. Rhodium catalyzed hydroformylation with BISBI gave high regioselectivity and fast rates for propene hydroformylation⁴ and for hexene hydroformylation¹² (n:i = 66.5:1, turnover rate = 12.4 [mol aldehyde] × [mol Rh]⁻¹ h⁻¹). The introduction of electron withdrawing groups on the aryl rings in BISBI-(3,5-CF₃) (**1**) led to a 2-fold increase in n:i regioselectivity and 5-fold faster rates (Table 2).

The T-BDCP ligand has a narrower bite angle than BISBI ($\beta_n = 106.6^\circ$ vs 112.6°), and a 37:63 mixture of **12-ee:12-ae** was observed for (T-BDCP)Ir(CO)₂H (**12**). Introduction of electron withdrawing groups on the aryl rings in T-BDCP-(3,5-CF₃) (**2**) led to an increased amount of diequatorial isomer of [T-BDCP-(3,5-CF₃)]Ir(CO)₂H (**13**) (**13-ee:13-ae** = 90:10). Rhodium catalyzed hydroformylation with T-BDCP-(3,5-CF₃) (**2**) led to an increase in n:i regioselectivity from 12.1 for T-BDCP to 17.7 for T-BDCP-(3,5-CF₃) (**2**). As in the case of BISBI, electron withdrawing substituents gave rise to increased n:i selectivity and to faster rates.

(28) The (chelate)(CO)₂IrH complexes of the *o*-tolyl and (*o*-trifluoromethyl)phenyl substituted DIPHOS derivatives also showed exclusive apical–equatorial coordination (see Supporting Information).

(29) Forster, D. *Inorg. Nucl. Chem. Lett.* **1969**, *5*, 433.

(30) Friebolin, H. *Basic One- and Two-Dimensional NMR Spectroscopy*; VCH Publishers: New York, 1993; p 295.

(31) Hydroformylation results for *o*-tolyl and (*o*-trifluoromethyl)phenyl substituted DIPHOS derivatives are given in Table 1 of Supporting Information.

The DIPHOS ligand has a narrow bite angle ($\beta_n = 84.5^\circ$) that leads to a strong preference for apical–equatorial coordination in (DIPHOS)Ir(CO)₂H. Rhodium catalyzed hydroformylation with DIPHOS gave relatively low *n*:*i* regioselectivity of 2.6:1. In contrast to the other two chelates, introduction of electron withdrawing substituents on the aryl rings in DIPHOS-(3,5-CF₃) (**3**) led to a *lower n:i regioselectivity* of 1.3:1 and to only a small rate increase.

Discussion

Wide bite angle diequatorial coordinating ligands like BISBI give high *n*:*i* regioselectivity of aldehyde formation in rhodium catalyzed hydroformylation, while apical–equatorial chelating ligands like DIPHOS give much lower *n*:*i* regioselectivity. Since our attempts to explain these differences in steric terms based on molecular mechanics calculations of model transition states failed to provide much insight, we initiated this study of electronic effects. Minor perturbations in the electronic properties of the ligands were made by introducing electron withdrawing groups on the aryl rings of the chelates.

The effect of electron withdrawing groups of equatorial phosphines was studied by comparing the regioselectivity obtained from BISBI and BISBI-(3,5-CF₃) (**1**). The 2-fold increase in regioselectivity achieved with electron withdrawing substituents is similar to the increases seen for ferrocenyl diphosphine chelates³² and for monodentate phosphines.³³ Unruh and Christenson studied the regioselectivity of rhodium catalyzed hydroformylation of 1-hexene using a series of 1,1'-bis(diarylphosphino)ferrocene ligands, which coordinate diequatorially.³⁴ They found a strong correlation between selectivity for linear aldehyde formation and the electron withdrawing ability of aryl substituents. Our results and Unruh's both demonstrate that electron withdrawing groups in the equatorial position lead to an increase in the *n*:*i* ratio. In less closely related work, RajanBabu reported that placing electron withdrawing substituents on arylphosphine chelates led to increased enantioselectivity in the hydroformylation of 2-vinylnaphthalenes.³⁵

The T-BDCP complexes exist as a mixture of diequatorial and apical–equatorial isomers. The addition of electron-withdrawing groups in T-BDCP-(3,5-CF₃) (**2**) shifted the equilibrium toward the diequatorial isomer. This shift to diequatorial coordination is consistent with Hoffmann's molecular orbital calculations that show a preference for equatorial coordination of σ -acceptor ligands.²⁷ The increase in *n*:*i* regioselectivity seen for T-BDCP-(3,5-CF₃) (**2**) may be due to two reinforcing effects. First, the increase in the amount of diequatorial chelation would be expected to favor linear aldehyde formation (high *n*:*i* for diequatorial BISBI). Second, the introduction of electron withdrawing aryl substituents in the diequatorial chelate should also enhance *n*:*i* selectivity as seen for BISBI-(3,5-CF₃) (**1**).

Mixtures of diequatorial and apical–equatorial isomers are also observed for monodentate phosphines. For example, Brown and Kent observed an 85:15 ratio of diequatorial and apical–equatorial isomers of (PPh₃)₂Rh(CO)₂H.¹⁰ In rhodium-catalyzed hydroformylation with triarylphosphine ligands bearing electron-withdrawing para substituents, Moser observed increased linear aldehyde regioselectivity and faster rates.³³ These trends can be explained by the same rationale used to account for the increased regioselectivity observed for T-BDCP-(3,5-CF₃) (**2**).

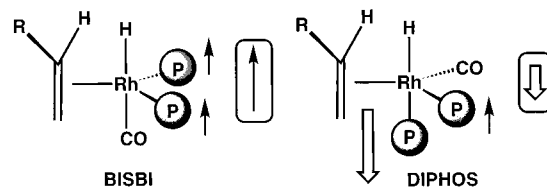


Figure 2. Effect of equatorial and apical electron withdrawing groups on *n*:*i* selectivity.

For PAR₃, electron-withdrawing groups are expected to increase the fraction of the diequatorial isomer that is expected to give more *n*-aldehyde. In addition, the presence of electron withdrawing groups in the diequatorial isomer should also lead to enhanced selectivity for *n*-aldehyde formation.

The influence on regioselectivity of electron withdrawing aryl groups on an apical phosphine cannot be measured directly and must be extracted from the selectivity observed with apical–equatorial chelating ligands. For the apical–equatorial bound DIPHOS ligand, we observed a *reduction* in the *n*:*i* ratio upon the addition of electron withdrawing groups. If electron withdrawing groups on the equatorial bound phosphine of DIPHOS-(3,5-CF₃) (**3**) increase the *n*:*i* ratio as seen for BISBI-(3,5-CF₃) (**1**), then electron withdrawing groups in the apical position of DIPHOS-(3,5-CF₃) (**3**) must *decrease* the *n*:*i* regioselectivity. Moreover, the negative influence of the apical phosphine must exceed the positive influence of the equatorial phosphine to obtain an overall decrease in the *n*:*i* ratio with DIPHOS-(3,5-CF₃) (**3**) (Figure 2). Our hypothesis then is that an electron withdrawing phosphine in the equatorial position increases the *n*:*i* ratio, while an electron withdrawing phosphine in the apical position decreases the *n*:*i* ratio.

A risky prediction of this hypothesis is that a dissymmetric DIPHOS derivative (Ar₂PCH₂CH₂PAR'₂) could lead to greater *n*:*i* selectivity than either of the related symmetric DIPHOS derivatives. A chelate designed to have an electron withdrawing phosphine in the equatorial position and a electron-donating phosphine in the apical position should give higher *n*:*i* regioselectivity than either of the parent symmetric DIPHOS compounds. We are currently pursuing an experimental test of this prediction.

Conclusion

Chelating diphosphines with electron withdrawing aryl substituents were synthesized and used in rhodium catalyzed hydroformylation of 1-hexene. Minor changes in the electronic character of phosphine ligands afforded significant changes in aldehyde regioselectivity. Interestingly, electron withdrawing groups in equatorial and apical positions had opposite effects on *n*:*i* regioselectivity. Hydroformylation results with the electron withdrawing *diequatorial* coordinated ligands BISBI-(3,5-CF₃) (**1**) and T-BDCP-(3,5-CF₃) (**2**) showed an increase in the *n*:*i* ratio, while *apical–equatorial* coordinated ligand DIPHOS-(3,5-CF₃) (**3**) showed a decrease in the *n*:*i* ratio. Thus, electron withdrawing aryl substituents in the equatorial position lead to higher *n*:*i* regioselectivity and in the apical position to lower regioselectivity.

However, a disturbing inconsistency emerges if the macroscopic changes in the catalyst upon going from BISBI to DIPHOS catalysts are considered. The macroscopic changes in going from H(alkene)Rh(CO)(BISBI) to H(alkene)Rh(CO)-(DIPHOS) involve replacement of an equatorial phosphine (one equatorial BISBI arm) with a strongly electron accepting CO ligand and replacement of an apical CO ligand by a strongly electron donating phosphine ligand (apical DIPHOS arm) (Figure 3). The second arm of each diphosphine, in the

(32) Unruh, J. D.; Christenson, J. R. *J. Mol. Catal.* **1982**, *14*, 19.

(33) Moser, W. R.; Papile, C. J.; Brannon, D. A.; Duwell, R. A.; Weininger, S. J. *J. Mol. Catal.* **1987**, *41*, 271.

(34) Hughes, O. R.; Young, D. A. *J. Am. Chem. Soc.* **1981**, *103*, 6636.

(35) RajanBabu, T. V.; Ayers, T. A. *Tetrahedron Lett.* **1994**, *35*, 4295.

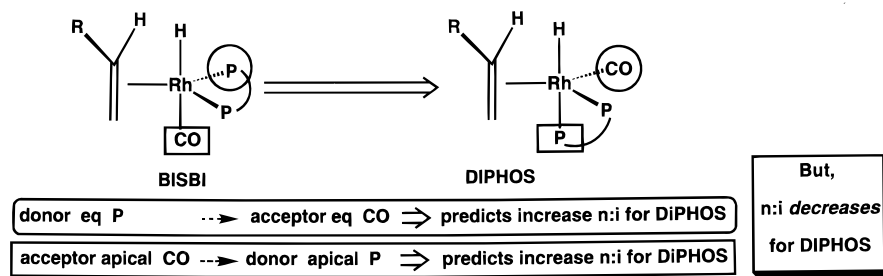


Figure 3. Predicted electronic effect of BISBI to DIPHOS substitution on *n:i* regioselectivity.

equatorial position, remains unchanged. Overall, the replacement of BISBI by DIPHOS places a better acceptor ligand in the equatorial position and a better donor ligand in the apical position. By analogy to the effect of electron donor aryl substituents, both of these changes should have resulted in higher regioselectivity not in the observed lower regioselectivity seen for DIPHOS.

Apparently, the major steric differences between diequatorial chelates like BISBI and apical–equatorial chelates like DIPHOS overwhelm any electron differences between the chelates. Clearly, the regioselectivity of hydroformylation is governed by a complex web of electronic and steric effects that have so far defied unraveling.

Experimental Section

General Methods. See Supporting Information. (3,5-(CF₃)₂C₆H₃)₂PCL,¹⁸ *t*-BDPC,³⁶ NBu₄[Ir(CO)₂L]₂,²⁹ (DIPHOS)Ir(CO)L,¹⁶ (Ph₃P)₃Ir(CO)H,³⁷ Ir(CO)₂(acac),³⁸ and Rh(CO)₂(acac)³⁹ were prepared by literature methods.

[3,5-(CF₃)₂C₆H₃]₂PH (4). Following a procedure similar to that used for diphenylphosphine,⁴⁰ a solution of [3,5-(CF₃)₂C₆H₃]₂PCL (17.5 g, 0.036 mol) in ether (200 mL) was slowly added to a suspension of LiAlH₄ (1.35 g, 0.036 mol) in ether (250 mL) at –78 °C. The pale brown slurry was refluxed for 2 h, cooled to 0 °C, and hydrolyzed with 10% aqueous NH₄Cl. The fluorescent yellow-green organic layer was separated, and the remaining white precipitate was extracted 5 times with ether. The combined ether extracts were washed with water, dried (Na₂SO₄), and evaporated to give **4** (12.6 g, 77%) as a pale yellow air-sensitive solid. Sublimation at 60 °C under vacuum gave **4** as a white solid, mp 69–71 °C. ¹H NMR (CD₂Cl₂, 300 MHz) δ 7.97 (d, *J*_{HP} = 6.5 Hz, ortho), 7.91 (s, para), 5.52 (d, *J*_{HP} = 225 Hz, PH). ¹³C{¹H} NMR (CD₂Cl₂, 75 MHz) δ 137.1 (d, *J*_{CP} = 15.8 Hz, ipso), 134.4 (d, *J*_{CP} = 18.4 Hz, ortho), 132.5 (qd, *J*_{CF} = 33.7 Hz, *J*_{CP} = 5.7 Hz, meta), 123.8 (br d, *J*_{CP} = 3.8 Hz, para), 123.6 (q, *J*_{CF} = 273 Hz, CF₃). ³¹P{¹H} NMR (CD₂Cl₂, 121 MHz) δ –40.2 (s). ¹⁹F{¹H} NMR (CD₂Cl₂, 282 MHz) δ –63.3 (s). IR (CCl₄): 2320 (ν_{P–H}); 1359, 1167, 1137 (ν_{CF}); 1279 (δ_{C=C–H}) cm^{–1}. HRMS Calcd (obsd) for C₁₆H₇F₁₂P 458.0094 (458.0086).

2,2'-Bis{[bis-{3,5-di(trifluoromethyl)phenyl}phosphino)methyl]-1,1'-biphenyl, BISBI-(3,5-CF₃) (1). Following a procedure similar to that used for (*R,R*)-*trans*-4,5-bis{[bis(2-trifluoromethylphenyl)phosphino)methyl]-2,2-dimethyl-1,3-dioxolane,⁴¹ 2,2'-bis(bromomethyl)-1,1'-biphenyl (370 mg, 1.09 mmol) in THF (10 mL) was added dropwise to a purple phosphide solution prepared from **4** (250 mg, 0.55 mmol) and KH (25 mg, 0.62 mmol) in THF (10 mL) at –78 °C. The reaction mixture was stirred overnight at room temperature. Solvent was evaporated and the residue was dissolved in Et₂O. The ether solution was washed with water, dried (Na₂SO₄), and evaporated

to give an oil. Recrystallization from EtOH gave **1** (650 mg, 54%) as a white solid, mp 133–138 °C. ¹H NMR (CD₂Cl₂, 300 MHz) δ 7.9–7.5 (m, aryl); 7.3–6.8 (m, biphenyl); 3.42, 3.26 (AB quartet, *J*_{AB} = 13 Hz, CH_AH_BP). ¹³C{¹H} NMR (CD₂Cl₂, 75.4 MHz) (note diastereotopic aryl groups) δ 141.0, 140.8, 140.7, 140.4 (all ipso C); 133.6 (br d, *J*_{CP} = 21 Hz, ortho-aryl(CF₃)₂); 132.8 (br d, *J*_{CP} = 18 Hz, ortho'-aryl(CF₃)₂); 132.3 (q, *J*_{CF} = 34 Hz, meta-aryl(CF₃)₂); 132.1 (q, *J*_{CF} = 33 Hz, meta'-aryl(CF₃)₂); 124.0 (sept, *J*_{CF} = 3 Hz para-aryl(CF₃)₂); 123.6 (sept, *J*_{CF} = 3 Hz para'-aryl(CF₃)₂); 133.9, 133.8, 131.0, 130.3, 130.2, 130.2, 128.6, 127.5 (other biphenyl and aryl); 123.5 (q, *J*_{CF} = 273 Hz, CF₃); 34.4 (d, *J*_{CP} = 20 Hz, CH₂P). ³¹P{¹H} NMR (CD₂Cl₂, 121 MHz) δ –8.5 (s). EI MS: *m/z* (%) 1094 (10) [P⁺], 1075 (17) [P⁺ – F].

trans-1,2-Bis{[bis-{3,5-di(trifluoromethyl)phenyl}phosphino)methyl]cyclopropane, T-BDCP-(3,5-CF₃) (2). Following a procedure similar to that used for **1**, *trans*-1,2-bis(tosyloxymethyl)cyclopropane⁴² (113 mg, 0.28 mmol) in THF (5 mL) was added to a phosphide solution prepared from **4** (250 mg, 0.55 mmol) and KH (25 mg, 0.62 mmol) in THF (4 mL) at –78 °C. Workup gave a clear oil that crystallized upon addition of EtOH to give **2** (100 mg, 36%) as a white solid, mp 110–112 °C. ¹H NMR (CD₂Cl₂, 300 MHz) δ 7.9–7.8 (m, aryl), 2.07 (m, CH₂P), 0.54 (m, 2H, CHCH₂P), 0.44 (m, cyclopropyl-CH₂). ³¹P{¹H} NMR (CD₂Cl₂, 121 MHz) δ –14.6 (s). ¹³C{¹H} NMR (CD₂Cl₂, 75.4 MHz) (note diastereotopic aryl groups) δ 141.3 (d, *J*_{CP} = 10 Hz, ipso), 141.1 (d, *J*_{CP} = 10 Hz, ipso'), 133.3 (d, *J*_{CP} = 18 Hz, ortho), 133.1 (d, *J*_{CP} = 18 Hz, ortho'), 132.3 (q, *J*_{CF} = 31 Hz, meta, meta'), 123.7 (s, para, para'), 123.6 (q, *J*_{CF} = 272 Hz, CF₃), 32.9 (d, *J*_{CP} = 13 Hz, CH₂P), 16.8 (dd, *J*_{CP} = 14, 12 Hz, CH), 15.8 (t, *J*_{CP} = 10 Hz, CH₂). LSIMS calcd (obsd) for C₃₇H₂₀F₂₄P₂ 982.5 (983.0).

[3,5-(CF₃)₂C₆H₃]₂P(CH=CH₂) (7). Following a procedure similar to that used for diphenylvinylphosphine,⁴³ a THF solution of vinyl magnesium bromide (70 mL, 1.0 M, 70 mmol) was added slowly to a benzene solution of [3,5-(CF₃)₂C₆H₃]₂PCL (21.0 g, 43 mmol). The solution was refluxed for 20 h and hydrolyzed with 100 mL of 10% aqueous NH₄Cl. The organic layer was separated, and the aqueous layer was extracted with ether and hot benzene. The combined organic layers were washed with water, dried (MgSO₄), and evaporated to give a brownish oil. High vacuum distillation of the oil from a 100 °C oil bath gave **7** as a white solid (9.7 g, 47%). ¹H NMR (CD₂Cl₂, 300 MHz) δ 7.94 (m, para), 7.90 (d, *J*_{HP} = 6.7 Hz, ortho), 6.71 (ddd, *J*_{HH} = 18.1, 11.5 Hz, *J*_{HP} = 7.4 Hz, CH=CH₂), 6.25 (ddd, *J*_{HP} = 38.2 Hz, *J*_{HH} = 11.5, 1.5 Hz, CH=CHH), 6.00 (ddd, *J*_{HH} = 18.1, 1.5 Hz, *J*_{HP} = 16.7 Hz, CH=CHH). ¹³C{¹H} NMR (CD₂Cl₂, 75 MHz) δ 141.1 (d, *J*_{CP} = 17 Hz, CH=CH₂), 135.4 (d, *J*_{CP} = 31 Hz, ipso), 133.65 (d, *J*_{CP} = 13 Hz, CH=CH₂), 133.4 (d, *J*_{CP} = 20 Hz, ortho), 132.7 (qd, *J*_{CF} = 33 Hz, *J*_{CP} = 6 Hz, meta), 123.9 (s, para), 123.8 (q, *J*_{CF} = 273 Hz, CF₃). ³¹P{¹H} NMR (121 MHz, CD₂Cl₂) δ –9.5 (s). ¹⁹F{¹H} NMR (CD₂Cl₂, 282 MHz) δ –63.3 (s). IR (CCl₄): 1616 (ν_{C=C}); 1354, 1187, 1146 (ν_{CF}); 1279 (δ_{C=C–H}) cm^{–1}.

1,2-Bis{[bis{3,5-di(trifluoromethyl)phenyl}phosphino)ethane, DIPHOS-(3,5-CF₃) (3). Following a procedure similar to that used for 1-diphenylphosphino-2-bis(*m*-fluorophenyl)phosphinoethane,⁴⁴ a mixture of **4** (5.0 g, 10.8 mmol), **7** (5.2 g, 10.8 mmol), and KO-*t*-Bu (0.2 g, 1.8 mmol) in THF (20 mL) was refluxed for 4 h. Solvent was

(36) Aviron-Violet, P.; Colleuille, Y.; Varagnat, J. *J. Mol. Cat.* **1979**, *5*, 41.

(37) Wilkinson, G. *Inorg. Synth.* **1972**, *13*, 126.

(38) Roberto, D.; Cariati, E.; Psaro, R.; Ugo, R. *Organometallics* **1994**, *13*, 4227.

(39) Varshavskii, Y. S.; Cherkasova, T. G. *Russ. J. Inorg. Chem.* **1967**, *12*, 899.

(40) Taylor, R. C.; Kolodny, R. and Walters, D. B. *Synth. Inorg. Met.-Org. Chem.* **1973**, *3*, 175.

(41) McKinsty, L.; Livinghouse, T. *Tetrahedron* **1994**, *50*, 6145.

(42) Blomquist, A. T.; Longone, D. T. *J. Am. Chem. Soc.* **1959**, *81*, 2012.

(43) Berlin, K. D.; Butler, G. B. *J. Org. Chem.* **1961**, *26*, 2537.

(44) Kapoor, P. N.; Pathak, D. D.; Gaur, G. and Kutty, M. *J. Organomet. Chem.* **1984**, *276*, 167.

evaporated, and the resulting brown residue was recrystallized twice from THF and then from CHCl_3 to give **3** (5.3 g, 52%) as a colorless solid, mp 178–182 °C. ^1H NMR (CD_2Cl_2 , 300 MHz) δ 7.91 (s, para), 7.78 (br s, ortho), 2.24 (virtual t, 10.5 Hz splitting, CH_2CH_2). $^{31}\text{P}\{^1\text{H}\}$ NMR (CD_2Cl_2 , 121 MHz) δ -10.7 (s). $^{19}\text{F}\{^1\text{H}\}$ NMR (CD_2Cl_2 , 282 MHz) δ -63.3 (s). EI MS: m/z (%) 942 (46) [M^+], 923 (24) [$\text{M}^+ - \text{F}$], 914 (35) [$\text{M}^+ - \text{C}_2\text{H}_4$].

[BISBI-(3,5-CF₃)₂Ir(CO)₂H (10)]. A CD_2Cl_2 solution of $\text{Ir}(\text{CO})_2$ -*(acac)* (3.2 mg, 9.2 μmol) and **1** (10 mg, 9.2 μmol) under 1 atm of 1:1 $\text{CO}:\text{H}_2$ was shaken in a NMR tube for 20 h to give a solution of **10**. ^1H NMR (CD_2Cl_2 , 300 MHz) δ 8.1–5.6 (m, aryl), 4.20 (dt, $J_{\text{HH}} = 13.5$ Hz, $J_{\text{HP}} = 3.4$ Hz, *PCHH*), 4.05 (dt, $J_{\text{HH}} = 13.5$, $J_{\text{HP}} = 7.5$ Hz, *PCHH*), -12.32 (t, $J_{\text{HP}} = 20$ Hz, Ir-H). $^{31}\text{P}\{^1\text{H}\}$ (CD_2Cl_2 , 121 MHz) δ 9.2 (s). $^{19}\text{F}\{^1\text{H}\}$ (CD_2Cl_2 , 282 MHz) δ -63.39 (s), -63.43 (s). ^1H NMR (CD_2Cl_2 , 300 MHz, -84 °C) δ 8.0–7.7 (m, 3,5-(CF_3)₂- C_6H_3), 7.4–6.9 (m, biphenyl), 6.0 (m, biphenyl), 4.25–3.8 (m, both $\text{CH}_A\text{H}_B\text{P}$), -12.54 (dd, $J_{\text{HP}} = 25$, 15 Hz, IrH). $^{31}\text{P}\{^1\text{H}\}$ (CD_2Cl_2 , 121 MHz, -84 °C) δ 13.28, 6.40 (ABq, $J_{\text{PP}} = 122$ Hz). IR (CH_2Cl_2): 2079 (w, $\nu_{\text{Ir-H}}$), 2005 (s, ν_{CO}), 1960 (vs, ν_{CO}) cm^{-1} .

(T-BDCP)Ir(CO)₂H (12). A solution of (T-BDCP)Ir(PPh_3)(CO)H (**11**) (334 mg, 0.362 mmol) in 6 mL of CH_2Cl_2 was stirred under 1 atm of CO at 25 °C for 2 days. Addition of 20 mL of a CO-saturated ethanol gave a precipitate which was immediately filtered and rinsed with ethanol to yield **12** (165 mg, 66%) as a white solid. ^1H NMR (CD_2Cl_2 , 500 MHz) δ 7.6–7.3 (m, aryl), 3.33 (m, CH_2P), 1.64 (m, CH), 0.64 (virtual t, 7 Hz splitting, CH_2), -11.48 (t, $J_{\text{HP}} = 16$ Hz, IrH). ^1H NMR (CD_2Cl_2 , 500 MHz, -74 °C) δ 7.6–7.3 (m, aryl), 3.33 (m, CH_2P), 1.64 (m, CH), 0.64 (virtual t, 7 Hz splitting, CH_2), -11.35 (dd, $J_{\text{HP}} = 97$, -23 Hz, IrH), -12.07 (dd, $J_{\text{HP}} = -26$, -15 Hz, IrH). $^{13}\text{C}\{^1\text{H}\}$ NMR (CD_2Cl_2) δ 183.5 (s, CO); 132.5 (t, $J_{\text{CP}} = 6$ Hz), 132.3 (t, $J_{\text{CP}} = 6$ Hz), 129.7 (d, $J_{\text{CP}} = 17$ Hz), 128.4 (m) (aryl); 38.8 (m, CH_2P); 19.3 (t, $J_{\text{CP}} = 8$ Hz, CH); 13.9 (t, $J_{\text{CP}} = 15$ Hz, CH_2). $^{31}\text{P}\{^1\text{H}\}$ (CD_2Cl_2) δ 1.3 (s). $^{31}\text{P}\{^1\text{H}\}$ (CD_2Cl_2 , -74 °C) δ 7.3 (d, $J_{\text{PP}} = 105$ Hz), 5.3 (d, $J_{\text{PP}} = 105$ Hz), 0.9 (d, $J_{\text{PP}} = 24$ Hz), -5.2 (d, $J_{\text{PP}} = 24$ Hz). IR (CH_2Cl_2): 2064 (m, $\nu_{\text{Ir-H}}$), 1970 (s, ν_{CO}), 1915 (s, ν_{CO}) cm^{-1} . IR (hexane) 1990 (s), 1978 (s), 1943 (vs), 1930 (vs) cm^{-1} .

[μ -BDCP-3,5-(CF₃)₂]Ir(CO)₂H (13). A CD_2Cl_2 solution of $\text{Ir}(\text{CO})_2$ -*(acac)* (4 mg, 11.5 μmol) and **2** (12 mg, 12.2 μmol) under 1 atm of 1:1 $\text{CO}:\text{H}_2$ was shaken in a NMR tube for 20 h to give a solution of **13**. ^1H NMR (CD_2Cl_2 , 300 MHz) δ 8.2–7.8 (m, aryl), 3.6 (m, CH_2P), 0.9 (m, 2H, *CHCH}_2\text{P}*), 0.6 (m, cyclopropyl- CH_2), -12.03 (t, $J_{\text{HP}} = 16$ Hz, IrH). $^{31}\text{P}\{^1\text{H}\}$ (CD_2Cl_2 , 121 MHz) δ 11.34 (s). $^{19}\text{F}\{^1\text{H}\}$ (CD_2Cl_2 , 282 MHz) δ -63.39 (s), -63.43 (s). ^1H NMR (CD_2Cl_2 , 300 MHz, -84 °C) δ 8.2–7.6 (m, aryl), 3.9 (m, *CHHP*), 3.4 (m, *CHHP*), 0.9 (m, 2H, *CHCH}_2\text{P}*), 0.5 (m, cyclopropyl- CH_2), -12.30 (dd, $J_{\text{HP}} = 28$, 17 Hz, IrH). $^{31}\text{P}\{^1\text{H}\}$ (CD_2Cl_2 , 121 MHz, -84 °C) δ 13.06, 10.78 (AB q, $J_{\text{PP}} = 116$ Hz). IR (CH_2Cl_2): 2064 (w, $\nu_{\text{Ir-H}}$), 2001 (s, ν_{CO}), 1955 (s, ν_{CO}) cm^{-1} .

[DIPHOS-(3,5-CF₃)₂]Ir(CO)₂H (15). Following a procedure similar to that used for (DIPHOS)Ir(CO)₂H,¹⁶ a benzene solution of [DIPHOS-(3,5-CF₃)₂]Ir(CO)H₃ (**17**) (80 mg, 0.067 mmol) in a quartz photolysis

cell purged with CO, was photolyzed for 30 min at 36 °C in a Rayonet photoreactor equipped with RPR 3000A bulbs with a maximum emission at 300 nm. The solvent was evaporated to give **15** (55 mg, 67%) as a pale yellow solid. ^1H NMR (CD_2Cl_2 , 500 MHz, 25 °C) δ 8.2–7.5 (m, aryl), 2.6 (m, CH_2P), -10.90 (t, $J_{\text{HP}} = 44$ Hz, IrH). ^1H NMR (CD_2Cl_2 , 500 MHz, -88 °C) δ -10.97 (dd, $J_{\text{HP}} = 101$, -14 Hz). $^{31}\text{P}\{^1\text{H}\}$ NMR (CD_2Cl_2 , 121 MHz, 25 °C) δ 39.8 (s). $^{31}\text{P}\{^1\text{H}\}$ (CD_2Cl_2 , 202 MHz, -96 °C): δ 39.0 (s), 37.5 (br s). ^{31}P NMR { ^1H decoupled, except for the hydride region} (CD_2Cl_2 , 202 MHz, 25 °C): δ 39.8 ($J_{\text{PH}} = 43$ Hz). ^{31}P { ^1H decoupled, except for the hydride region} (CD_2Cl_2 , 202 MHz, -98 °C) δ 39.2 (br s), 37.4 (br d, $J_{\text{PH}} = 103$ Hz). $^{19}\text{F}\{^1\text{H}\}$ NMR (CD_2Cl_2 , 282.2 MHz, 25 °C) δ -63.38 (s). IR (CH_2Cl_2) 2002, 1954 cm^{-1} .

Catalytic Hydroformylation of 1-Hexene. Hydroformylation reactions were performed as described earlier in a 90-mL Fischer-Porter bottle equipped with a star-head magnetic stir bar.¹² $\text{Rh}(\text{CO})_2$ (*acac*) (10 mg, 0.03875 mmol) and a chelating diphosphine (0.03875 mmol) were dissolved in benzene (6.0 mL) under 70 psig of analyzed $\text{CO}:\text{H}_2$ (50.02% CO, 49.98% H_2) with toluene (0.20 mL, 1.9 mmol) added as an internal GC standard. After 1 h of stirring at 34 ± 2 °C, 1-hexene (2.50 mL, 0.020 mmol) was added. Samples containing heptanal and 2-methylhexanal were analyzed by temperature-programmed gas chromatography on an HP5890A chromatography interfaced to a HP3390A integrator using an HP-1 10 m \times 0.53 mm methyl silicone gum capillary column.

Acknowledgment. Financial support from the Department of Energy, Office of Basic Energy Sciences, is gratefully acknowledged. E.W.B. thanks the Fulbright commission for a fellowship. B.R.P. thanks the Alexander von Humboldt Stiftung for a von Lynene Fellowship. Grants from NSF (CHE-9105497) and from the University of Wisconsin for the purchase of the X-ray instruments and computers are acknowledged. We thank Alpha Aesar for a loan of iridium compounds.

Supporting Information Available: General experimental methods and experimental details and characterization for **8**, **9**, **11**, **14**, **17**, (2- $\text{CH}_3\text{C}_6\text{H}_4$)₂P(O)H, (2- $\text{CF}_3\text{-C}_6\text{H}_4$)₂P(O)H, (2- $\text{CH}_3\text{C}_6\text{H}_4$)₂P(O)Cl, (2- $\text{CF}_3\text{-C}_6\text{H}_4$)₂P(O)Cl, (2- $\text{CH}_3\text{C}_6\text{H}_4$)₂P($\text{CH}=\text{CH}_2$), (2- $\text{CF}_3\text{-C}_6\text{H}_4$)₂P($\text{CH}=\text{CH}_2$), (2- $\text{CH}_3\text{C}_6\text{H}_4$)₂PH, (2- $\text{CF}_3\text{C}_6\text{H}_4$)₂PH, (2- $\text{CH}_3\text{C}_6\text{H}_4$)₂PCH₂CH₂P(2- $\text{CH}_3\text{C}_6\text{H}_4$)₂ (**DIPHOS-(2-CH₃)**), (2- $\text{CF}_3\text{C}_6\text{H}_4$)₂PCH₂CH₂P(2- $\text{CF}_3\text{C}_6\text{H}_4$)₂ (**DIPHOS-(2-CF₃)**), [T-BDCP-(3,5-CF₃)₂]Ir(PPh_3)(CO)H, [DIPHOS-(3,5-CF₃)₂]Ir(CO)I, [DIPHOS-(2-CH₃)₂]Ir(CO)I, [DIPHOS-(2-CF₃)₂]Ir(CO)I, [DIPHOS-(2-CH₃)₂]Ir(CO)H₃, [DIPHOS-(2-CF₃)₂]Ir(CO)H₃, and [DIPHOS-(2-CH₃)₂]Ir(CO)H₂ and [DIPHOS-(2-CF₃)₂]Ir(CO)₂H and X-ray crystallographic data for **9** (26 pages). See any current masthead page for ordering and Internet access instructions.

JA9719440